

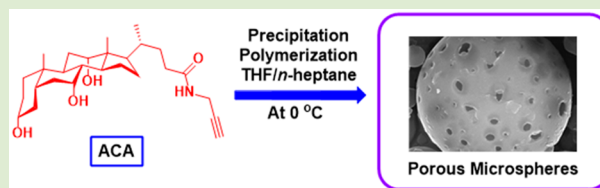
# Optically Active Porous Microspheres Consisting of Helical Substituted Polyacetylene Prepared by Precipitation Polymerization without Porogen and the Application in Enantioselective Crystallization

Chunni Chen,<sup>†,‡,§</sup> Biao Zhao,<sup>†,‡,§</sup> and Jianping Deng<sup>\*,†,‡</sup>

<sup>†</sup>State Key Laboratory of Chemical Resource Engineering and <sup>‡</sup>College of Materials Science and Engineering, Beijing University of Chemical Technology, Beijing 100029, China

## S Supporting Information

**ABSTRACT:** A novel chiral acetylenic monomer derived from cholic acid was synthesized and structurally characterized. The monomer underwent precipitation polymerization in tetrahydrofuran/*n*-heptane mixed solvent with [Rh(nbd)Cl]<sub>2</sub> as catalyst. Without adding porogen, porous microspheres were successfully prepared in a high yield (>80 wt %). The formation mechanism of the porous structure was proposed. Circular dichroism and UV–vis absorption spectra demonstrated that the porous microspheres possessed optical activity. The optical activity was originated in the chiral helical conformations of substituted polyacetylene forming the microspheres. The porous microspheres were further used as specific chiral additive to induce enantioselective crystallization of racemic BOC-alanine, in which BOC-L-alanine was preferentially induced forming rod-like crystals with e.e. of 69%. This strongly indicates the significant potential applications of the porous microspheres in chiral technologies. The present study also provides a new approach to prepare chiral porous polymer microspheres.



As a natural compound, cholic acid (CA) possesses unique structure and exhibits interesting facial amphiphilicity in which the  $\alpha$ -face is hydrophilic and the  $\beta$ -face is hydrophobic.<sup>1</sup> The feature endows CA with significant potential applications as biocompatible materials.<sup>2</sup> Also remarkably, the multifunctional groups of CA can be modified to synthesize biocompatible polymers with CA in polymer main chains,<sup>3,4</sup> pendant groups,<sup>5,6</sup> or chain end groups.<sup>7,8</sup> Additionally, a variety of monomers were prepared by the interaction of CA with other functional groups, such as methacrylate<sup>9</sup> and acryl(meth)amide group.<sup>10</sup> Massive polymers based on CA have been reported in recent years, such as self-healing supramolecular hydrogels,<sup>9</sup> biodegradable polymer microspheres,<sup>11</sup> and functional star polymers bearing CA pendant groups.<sup>12</sup> Thermo- and pH-responsible polymers containing CA moieties were also synthesized.<sup>13</sup> Reportedly, CA monomers functionalized with both alkyne and azide groups can be used to prepare main-chain poly(cholic acid).<sup>14</sup> Unfortunately, the chirality of CA has hardly been exploited yet. The present article reports for the first time a novel type of chiral helical polymer microspheres derived from CA.

Chiral polymer particles (CPPs) are currently gathering ever-increasing attention because of their outstanding properties, such as intriguing optical activity, large specific surface area, and small size, which endow CPPs with huge potential applications in chiral recognition/resolution,<sup>15</sup> asymmetric catalysis,<sup>16</sup> enantioselective crystallization,<sup>17</sup> enantioselective-controlled release,<sup>18</sup> and so on. The CPPs constructed by chiral helical

polymers are especially attractive.<sup>19–32</sup> Generally, CPPs can be formed via diverse methods for example self-assembly.<sup>33–39</sup> Deng group has successfully prepared a series of CPPs through emulsion polymerization,<sup>40–42</sup> precipitation polymerization,<sup>43,44</sup> and suspension polymerization<sup>45–47</sup> approaches. As an important branch of CPPs, chiral porous polymer particles are particularly intriguing because of their prominent properties, including higher surface area, well-defined porosity, and lower density. In recent years, various porous polymer particles<sup>48–51</sup> and chiral hollow polymer particles<sup>16,42</sup> have been established. Nonetheless, chiral porous polymer particles have been scarcely reported yet.

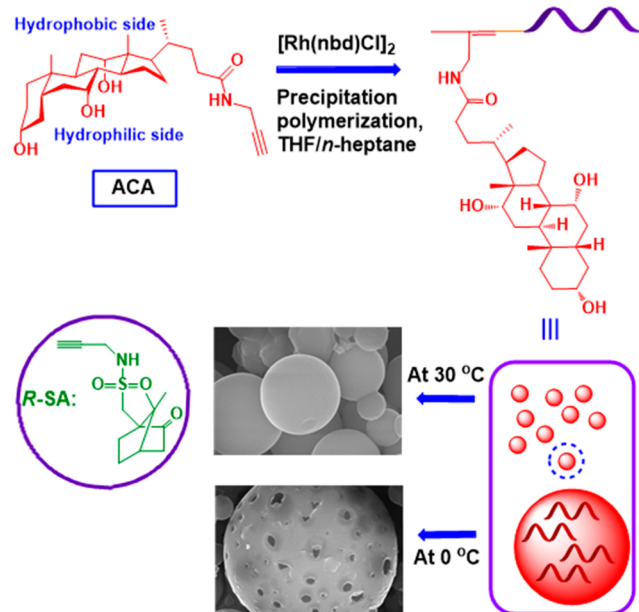
In this contribution, we created a new approach for preparing chiral porous polymer microspheres (CPPMs) via precipitation polymerization. We first synthesized an acetylenic monomer derived from cholic acid (CA) following a well-investigated strategy.<sup>52</sup> Then we prepared the anticipated porous chiral microspheres by taking the precipitation polymerization methodology developed by us previously.<sup>43,44</sup> Porous polymer microspheres were fabricated under appropriate polymerization conditions (Scheme 1). We highlight that the CPPMs were fabricated without adding specific porogen. According to the present investigations and also referring to our earlier studies,<sup>43,44</sup> we subsequently propose a formation mechanism

Received: February 4, 2015

Accepted: March 9, 2015

Published: March 11, 2015

### Scheme 1. Illustrative Strategy for Preparing Chiral Porous Microspheres (CPPMs) by Precipitation Polymerization



for the CPPMs. Finally, the resulting CPPMs were used as specific chiral additives for inducing enantioselective crystallization by using BOC-alanine as model chiral compounds.

In the present study, a novel substituted acetylene monomer (ACA) with cholic acid unit was synthesized by a well-investigated approach,<sup>52</sup> as presented in Scheme S1. The monomer was obtained in a 80 wt % yield and then characterized by FT-IR and NMR spectroscopies, as shown in Figures S1 and S2 (in Supporting Information). The detailed analyses are described therein, confirming the successful production of the monomer. To acquire more understanding of the monomer ACA and the corresponding polymer, ACA first underwent solution polymerization in methanol as solvent. GPC was utilized to analyze the molecular weight and molecular weight distribution of the obtained polymer (PACA). The number-average molecular weight ( $M_n$ ) of PACA is 33200 g/mol and the molecular weight distribution ( $M_w/M_n$ ) is 2.90. The solubility of the monomer and polymer was tested and presented in Table S1. DSC (Figure S3 in Supporting Information) and TGA (Figure S4) analyses show that the glass transition temperature ( $T_g$ ) and temperature for maximum decomposition rate ( $T_d$ ) of PACA are 175 and 493 °C, respectively. The results demonstrate that the polymer possess good thermal performance.

According to our previous research,<sup>43</sup> precipitation polymerization has been proved to be an ideal process to prepare pure chiral polymer particles. Compared to other polymerization methods, like emulsion polymerization, precipitation polymerization is much easier to operate and in particular can provide pure polymer particles. In the present research, monomer ACA underwent precipitation polymerization in tetrahydrofuran (THF)/*n*-heptane solvent mixture. To explore the optimal reaction system for preparing regular microspheres, the effects of the solvent mixture in varied ratio of THF/*n*-heptane were examined. The polymerizations took place in the presence of Rh complex at 30 °C for 4 h. The SEM images (Figure S5) demonstrate that polymer microspheres with rather regular morphology and relatively narrow disperse were obtained with

THF/*n*-heptane = 1/5 (mL/mL). The  $M_n$  of PACA chains constructing the microsphere is 24500 and the  $M_n/M_w$  is 1.28 (Figure S6).

Notably, an interesting phenomenon was observed when the polymerization temperature was changed. The SEM images of microspheres prepared at different temperatures are shown in Figure 1. Microspheres with remarkable pores were fabricated

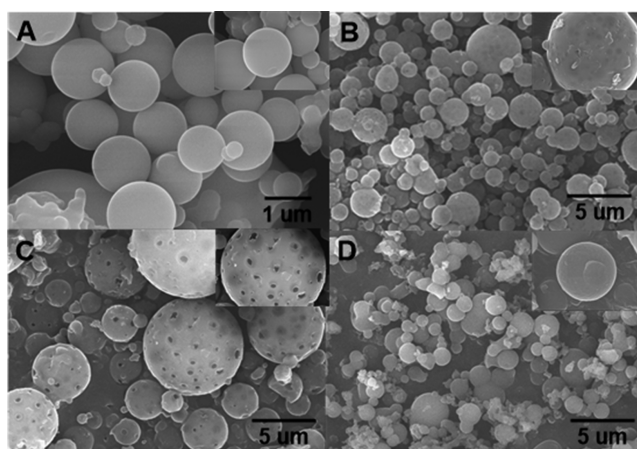
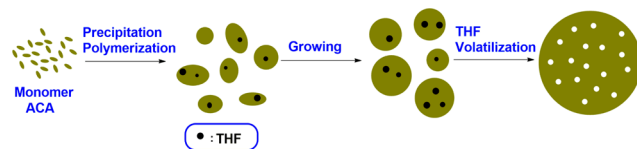


**Figure 1.** SEM images of chiral PACA microspheres prepared by precipitation polymerization of ACA in THF/*n*-heptane (1/5, mL/mL) at varied temperature: A, 30 °C; B, 10 °C; C, 0 °C; D, -10 °C.

when the precipitation polymerization was carried out at 0 °C (Figure 1C). Precipitation polymerization at other temperatures (30, 10, and -10 °C) failed to provide microspheres with pores. To further elucidate the formation mechanism of the porous microspheres, we tried another acetylenic monomer R-SA (also structurally presented in Scheme 1). When monomer SA underwent precipitation polymerization at 0 °C under similar conditions for monomer ACA, the resulting microspheres did not possess pores, as observed in the relevant SEM images (Figure S7). Accordingly, we attribute the formation of porous structures in the microspheres to the special cholic acid moieties.

To further discuss the forming process of porous microspheres vividly, a schematic representation is illustrated in Scheme 2. In the progress of precipitation polymerization, the

### Scheme 2. Schematic Illustration of the Porous Microspheres Formation Process



formed polymer chains, when grown to a certain length, were precipitated out and aggregated, resulting in the nucleation sites. Polymer chains continuously aggregated on the nucleation sites in the course of polymerization, and the diameter of the microspheres increased gradually. As more polymer chains aggregated around the preformed nucleation sites (cores), spherical products were formed finally. Importantly, growing of the microsphere was accompanied by phase separation of THF from the original homogeneous solvent mixture, due to the relatively higher affinity of the polymer chains to THF (the

relatively good solvent for the polymer chains, while *n*-heptane is the poor solvent). After the formation of the microspheres, THF domains still left inside the microspheres, as shown in Scheme 2. Eventually, porous structures were fabricated with the volatilization of THF. This strategy is in theory applicable for other types of polymers, besides acetylenic polymers.

Substituted polyacetylenes can form helical conformations under appropriate conditions, for example, forming intramolecular hydrogen bonding,<sup>20,21,29</sup> undergoing solvophobic effect,<sup>53</sup> and complexing with metal ions.<sup>25,26</sup> Moreover, cis-structures in polyacetylenes facilitated the polymer chains to form helical structures.<sup>54</sup> According to our previous studies,<sup>41,55</sup> circular dichroism (CD) and UV–vis absorption spectroscopy techniques have been proved highly efficient to analyze the secondary structures of substituted polyacetylenes. The predominant helicity of substituted polyacetylenes can be reflected by CD signals. To investigate the optical activity of the porous microspheres obtained above, we characterized them by CD and UV–vis absorption spectroscopies. The CD and UV–vis spectra are presented in Figure 2. Obvious CD signal around

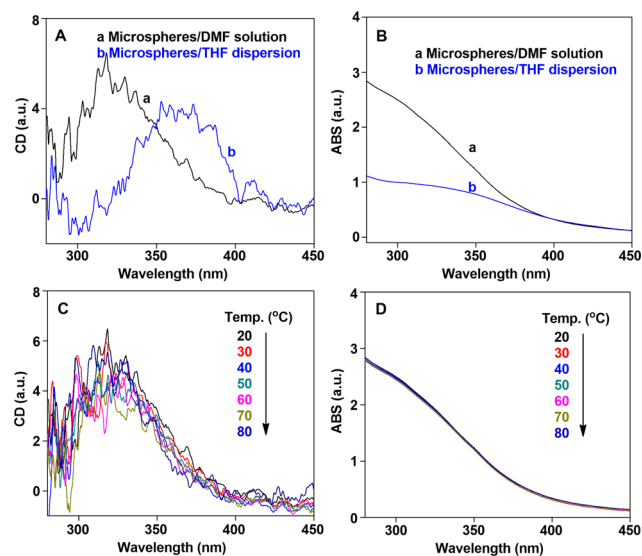


**Figure 2.** CD (A) and UV–vis (B) spectra of porous microspheres: a and b, porous microspheres dissolved in DMF and dispersed in THF, respectively. Temperature dependence of CD (C) and UV–vis (D) spectra of PACA microspheres dissolved in DMF.

320 nm was observed when the porous microspheres were dissolved in DMF (Figure 2A). This CD effect indicates the formation of helical conformations in the polymer chains.<sup>40,41,55</sup> In the UV–vis spectra in Figure 2B, an absorption peak is also found at 320 nm, similar to the CD spectra. To keep well the spheric morphology of the porous microspheres in the course of measurements, we recorded CD and UV–vis spectra by dispersing the microspheres in THF. The obtained spectra in this case are illustrated in Figure 2A. CD effect is also observed as expected. On the basis of our earlier intensive studies dealing with helical polyacetylene-based particles,<sup>40–43,55</sup> we conclude that the CD effects demonstrate the polymer chains in the microspheres adopting helical structures with predominant helicity. Furthermore, the microspheres possess optical activity.

The stability of the polymer helical structures was further explored by measuring CD and UV–vis absorption spectra at different temperature. The recorded spectra are shown in Figure 2C,D. When the temperature increased from 20 to 80

°C, the CD signals changed little and the UV–vis absorption also remained constant. Generally, the increase of temperature leads to conformational transition between ordered polymeric helical structures and disordered structures or between right- and left-handed helices.<sup>51</sup> For the present polymers (PACA), the pendant groups of ACA occupy a large space, and the conformational transition of polymer chains is strongly limited. The above results demonstrate that PACA microsphere in solution can keep stable macromolecular helical conformations at high temperature.

Optically active polymers are expected to find significant applications in chiral resolution. With the chiral porous polymer microspheres (CPPMs) in hand, we next utilized them as a specific chiral additive for performing enantioselective crystallization. For this purpose, we utilized BOC-alanine as model chiral compounds to be separated. Excitingly, we found that the porous PACA microspheres preferably induced one of the BOC-alanine enantiomers to crystallize. To obtain a deeper understanding of the induced crystallization, crystallization of racemic BOC-alanine solution was performed under similar conditions but in the absence of any additive. The SEM images of the crystals induced by CPPMs toward racemic BOC-alanine are presented in Figure 3. Crystals obtained with or without

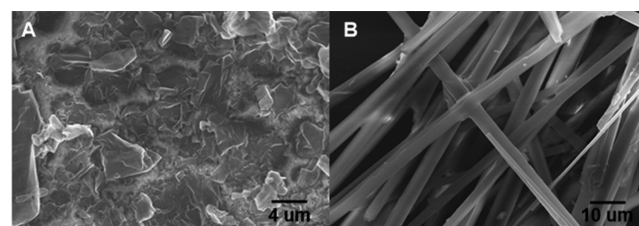


**Figure 3.** SEM images of BOC-alanine crystals obtained via enantioselective crystallization: (A) without additive and (B) by using porous PACA microspheres as chiral additive.

porous PACA microspheres present different morphologies. For the BOC-alanine crystals obtained without any additive, bulks (Figure 3A) without regular morphology and size were obtained. For the BOC-alanine crystals obtained by using porous PACA microspheres as the chiral additive, beautiful rod-like crystals with regular morphology were obtained, as shown in Figure 3B. Moreover, the rod-like crystals were experimentally proved to be predominantly constructed by BOC-L-alanine, as to be discussed later. The rod-like crystals of BOC-L-alanine obtained via enantioselective crystallization were subjected to XRD analyses, and the obtained XRD patterns are illustrated in Figure S8. The XRD patterns of pure BOC-L-alanine are also presented for a clear comparison. The two patterns are almost entirely the same, demonstrating the same crystalline structure between the pure and the induced crystals.

To acquire deeper insights into the enantioselective crystallization by the porous PACA microspheres, we further characterized the obtained crystals with CD spectroscopy, as presented in Figure S9. A comparison of pure BOC-L-alanine, the residual solution after crystallization and the crystals induced by porous PACA microspheres are presented in Figure S9. The results indicate the rod-like BOC-alanine crystals obtained by using porous PACA microspheres as additive are predominantly formed by BOC-L-alanine, providing further evidence for the conclusion that enantioselective crystallization was realized in the presence of porous PACA microspheres. The chiral resolution efficiency (e.e., enantio-

meric excess) in the enantioselective crystallization process was subsequently investigated, which was determined by measuring the optical rotation of the residual solution as a function of time in the course of enantioselective crystallization. The maximum chiral resolution was achieved after 72 h, and the e.e. (determined by the ratio of the optical rotation of the residual solution to the optical rotation of the pure sample solution) in this case could be as high as 69%. The optical rotation of the residual solution was found to be in positive sign (attributed to BOC-D-alanine), further demonstrating that BOC-L-alanine was preferentially induced to crystallize by the porous PACA microspheres.

In conclusion, we synthesized a chiral substituted acetylene monomer derived from cholic acid. Chiral porous polymer microspheres (CPPMs) were prepared in high yield when the monomer underwent precipitation polymerization in the presence of Rh-catalyst in THF/*n*-heptane (1/5, v/v) at 0 °C. The CPPMs exhibited considerable optical activity constructed by helical polymer chains of one predominant screw sense. The helical structures showed relatively higher thermal stability. CPPMs efficiently induced enantioselective crystallization of racemic BOC-alanine enantiomers. The present investigations developed a new strategy to prepare chiral porous polymer microspheres. They are of high interest due to potential applications like chiral resolution. After optimization in composition and morphology, the chiral porous microspheres may find significant applications in asymmetric catalysis as chiral catalyst. Our investigations along these attractive research directions are currently ongoing.

## ■ ASSOCIATED CONTENT

### Supporting Information

Materials, experimental details, and supplementary data. This material is available free of charge via the Internet at <http://pubs.acs.org>.

## ■ AUTHOR INFORMATION

### Corresponding Author

\*E-mail: [dengjp@mail.buct.edu.cn](mailto:dengjp@mail.buct.edu.cn).

### Author Contributions

<sup>§</sup>These authors contributed equally (C.C. and B.Z.).

### Notes

The authors declare no competing financial interest.

## ■ ACKNOWLEDGMENTS

This work was supported by the National Natural Science Foundation of China (21474007, 21274008, 21174010), the Funds for Creative Research Groups of China (51221002), and the "Specialized Research Fund for the Doctoral Program of Higher Education" (SRFDP 20120010130002).

## ■ REFERENCES

- (1) Kramer, W.; Wess, G.; Enhsen, A.; Falk, E.; Hoffmann, A.; Nechermann, G.; Schubert, G.; Urman, M. *J. Controlled Release* **1997**, *46*, 17–30.
- (2) Li, W. N.; Li, X. S.; Zhu, W.; Li, C. X.; Xu, D.; Ju, Y.; Li, G. T. *Chem. Commun.* **2011**, *47*, 7728–7730.
- (3) Zhang, X. D.; Dong, Y. C.; Zeng, X. W.; Liang, X.; Li, X. M.; Tao, W.; Chen, H. B.; Jiang, Y. Y.; Mei, L.; Feng, S. *Biomaterials* **2014**, *35*, 1932–1943.
- (4) Li, W. N.; Tian, T.; Zhu, W.; Cui, J. C.; Ju, Y.; Li, G. T. *Polym. Chem.* **2013**, *4*, 3057–3068.

- (5) Du, H. L.; Yang, X. Y.; Pang, X.; Zhai, G. X. *Carbohydr. Polym.* **2014**, *111*, 753–761.
- (6) Bai, G. Y.; Wang, Y. J.; Marieta, N.; Margarida, B. *Langmuir* **2013**, *29*, 13258–13268.
- (7) Doganci, E.; Gorur, M.; Uyanik, C.; Yilmaz, F. *J. Polym. Sci., Part A: Polym. Chem.* **2014**, *52*, 3390–3399.
- (8) Zeng, X. W.; Tao, W.; Mei, L.; Huang, L. Q.; Tan, C. Y. *Biomaterials* **2013**, *34*, 6058–6067.
- (9) Jia, Y. G.; Zhu, X. X. *Langmuir* **2014**, *30*, 11770–11775.
- (10) Liu, H. Y.; Avoce, D.; Song, Z. J.; Zhu, X. X. *Macromol. Rapid Commun.* **2001**, *22*, 675–680.
- (11) Fu, H. L.; Li, Y. Q.; Shao, L.; Cheng, S. X.; Zhang, X. Z.; Zhuo, R. X. *J. Microencapsulation* **2010**, *27*, 345–354.
- (12) Doganci, E.; Gorur, M.; Uyanik, C.; Yilmaz, F. *J. Polym. Sci., Part A: Polym. Chem.* **2014**, *52*, 3390–3399.
- (13) Sunirmal, P.; Saswati, G. R.; Priyadarsi, D. *Polym. Chem.* **2014**, *5*, 1275–1284.
- (14) Li, W. N.; Li, X. S.; Zhu, W.; Li, C. X.; Xu, D.; Ju, Y.; Li, G. T. *Chem. Commun.* **2011**, *47*, 7728–7730.
- (15) Paik, P.; Gedanken, A.; Mastai, Y. *J. Mater. Chem.* **2010**, *20*, 4085–4093.
- (16) Thvedt, T. H. K.; Kristensen, T. E.; Sundby, E.; Hansen, T.; Hoff, B. H. *Tetrahedron: Asymmetry* **2011**, *22*, 2172–2178.
- (17) Medina, D. D.; Goldshtein, J.; Margel, S.; Mastai, Y. *Adv. Funct. Mater.* **2007**, *17*, 944–950.
- (18) Liu, D.; Chen, H. Y.; Deng, J. P.; Yang, W. T. *J. Mater. Chem. C* **2013**, *1*, 8066–8074.
- (19) Jain, V.; Cheon, K. S.; Tang, K.; Jha, S.; Green, M. M. *Isr. J. Chem.* **2011**, *51*, 1067–1074.
- (20) Liu, J. C.; Lam, J. W. Y.; Tang, B. Z. *Chem. Rev.* **2009**, *109*, 5799–5867.
- (21) Yashima, E.; Maeda, K.; Iika, H.; Furusho, Y.; Nagai, K. *Chem. Rev.* **2009**, *109*, 6102–6211.
- (22) Rudick, J. G.; Percec, V. *Acc. Chem. Res.* **2008**, *41*, 1641–1652.
- (23) Pietropaolo, A.; Nakano, T. *J. Am. Chem. Soc.* **2013**, *135*, 5509–5512.
- (24) Yoshida, Y.; Mawatari, Y.; Motoshige, A.; Motoshige, R.; Hiraoki, T.; Wagner, M.; Müllen, K.; Tabata, M. *J. Am. Chem. Soc.* **2013**, *135*, 4110–4116.
- (25) Freire, F.; Seco, J. M.; Quiñoá, E.; Riguera, R. *J. Am. Chem. Soc.* **2012**, *134*, 19374–19383.
- (26) Bergueiro, J.; Freire, F.; Wendler, E. P.; Seco, J. M.; Quiñoá, E.; Riguera, R. *Chem. Sci.* **2014**, *5*, 2170–2176.
- (27) Budhathodi-Uprety, J.; Novak, B. M. *Macromolecules* **2011**, *44*, 5947–5954.
- (28) Zhang, C. H.; Wang, H. L.; Geng, Q. Q.; Yang, T. T.; Liu, L. J.; Sakai, R.; Satoh, T.; Kakuchi, T.; Okamoto, Y. *Macromolecules* **2013**, *46*, 8406–8415.
- (29) Shiotsuki, M.; Sanda, F.; Masuda, T. *Polym. Chem.* **2011**, *2*, 1044–1058.
- (30) Jia, H.; Teraguchi, M.; Aoki, T.; Abe, Y.; Akaneko, T.; Hadano, S.; Namikoshi, T.; Ohishi, T. *Macromolecules* **2010**, *43*, 8353–8362.
- (31) Wulff, G.; Poll, H. J.; Milan, M. *J. Liq. Chromatogr.* **1986**, *9*, 385–405.
- (32) *Materials-Chirality*; Green, M. M., Nolte, R. J. M., Meijer, E. W., Eds.; John Wiley & Sons, Inc., Hoboken, NJ, U.S.A., 2003; Vol. 24.
- (33) Guenet, J.-M.; Jeon, H. S.; Khatri, C.; Jha, S. K.; Balsara, N. P.; Green, M. M.; Brület, A.; Thierry, A. *Macromolecules* **1997**, *30*, 4590–4596.
- (34) Goto, H.; Okamoto, Y.; Yashima, E. *Macromolecules* **2002**, *35*, 4590–4601.
- (35) Zhao, L. Z.; Ma, R. J.; Li, J. B.; Li, Y.; An, Y. L.; Shi, L. Q. *Biomacromolecules* **2008**, *9*, 2601–2608.
- (36) Peng, W. Q.; Motonaga, M.; Koe, J. R. *J. Am. Chem. Soc.* **2004**, *126*, 13822–13826.
- (37) Cipparrone, G.; Mazzulla, A.; Pane, A.; Hernandez, R. J.; Bartolino, R. *Adv. Mater.* **2011**, *23*, 5773–5778.
- (38) Watanabe, K.; Iida, H.; Akagi, K. *Adv. Mater.* **2012**, *24*, 6451–6456.

- (39) Nakano, Y.; Fujiki, M. *Macromolecules* **2011**, *44*, 7511–7519.
- (40) Deng, J. P.; Chen, B.; Luo, X. F.; Yang, W. T. *Macromolecules* **2009**, *42*, 933–938.
- (41) Luo, X. F.; Deng, J. P.; Yang, W. T. *Angew. Chem., Int. Ed.* **2011**, *50*, 4909–4912.
- (42) Chen, B.; Deng, J. P.; Yang, W. T. *Adv. Funct. Mater.* **2011**, *21*, 2345–2350.
- (43) Zhang, D. Y.; Song, C.; Deng, J. P.; Yang, W. T. *Macromolecules* **2012**, *45*, 7329–7338.
- (44) Huang, H. J.; Chen, C. N.; Zhang, D. Y.; Deng, J. P.; Wu, Y. P. *Macromol. Rapid Commun.* **2014**, *35*, 908–915.
- (45) Song, C.; Zhang, C. H.; Wang, F. J.; Yang, W. T.; Deng, J. P. *Polym. Chem.* **2013**, *4*, 645–652.
- (46) Zhang, H. Y.; Song, J. X.; Deng, J. P. *Macromol. Rapid Commun.* **2014**, *35*, 1216–1223.
- (47) Liang, J. Y.; Song, C.; Deng, J. P. *Appl. Mater. Interfaces.* **2014**, *6*, 19041–19049.
- (48) Xie, B. Q.; Shi, H. F.; Liu, G. M.; Zhou, Y.; Wang, Y.; Zhao, Y.; Wang, D. J. *Chem. Mater.* **2008**, *20*, 3099–3104.
- (49) Takai, C.; Hotta, T.; Shiozaki, S.; Boonsongrit, Y.; Abe, H. *Chem. Commun.* **2009**, *37*, 5533–5535.
- (50) Kim, M. R.; Lee, S.; Park, J. K.; Cho, K. Y. *Chem. Commun.* **2010**, *46*, 7433–7435.
- (51) Yu, Q. B.; Tao, Y. L.; Huang, Y. P.; Lin, Z. Q.; Zhuang, Y. L.; Ge, L. L.; Shen, Y. H.; Hong, M.; Xie, A. *Ind. Eng. Chem. Res.* **2012**, *51*, 8117–8122.
- (52) Deng, J. P.; Tabei, J.; Shiotsuki, M.; Sanda, F.; Masuda, T. *Macromolecules* **2004**, *37*, 1891–1896.
- (53) Percec, V.; Peterca, M.; Rudick, J. G.; Aqad, E.; Imam, M. R.; Heiney, P. A. *Chem.—Eur. J.* **2007**, *13*, 9572–9581.
- (54) Simionescu, C. I.; Percec, V.; Dumitrescu, S. J. *Polym. Sci., Part A: Polym. Chem.* **1977**, *15*, 2497–2509.
- (55) Chen, B.; Deng, J. P.; Liu, X. Q.; Yang, W. T. *Macromolecules* **2010**, *43*, 3177–3182.